

Mass Varying Neutrinos in the Sun

Marco Cirelli*

Physics Dept. - Yale University, New Haven, CT 06520, USA

M.C. Gonzalez-Garcia[†]

*C.N. Yang Institute for Theoretical Physics,
SUNY at Stony Brook, Stony Brook, NY 11794-3840, USA
IFIC, Universitat de València - C.S.I.C.,
Apt 22085, E-46071 València, Spain*

Carlos Peña-Garay[‡]

School of Natural Sciences, Institute for Advanced Study, Princeton, NJ 08540, USA

Abstract

In this work we study the phenomenological consequences of the dependence of mass varying neutrinos on the neutrino density in the Sun, which we precisely compute in each point along the neutrino trajectory. We find that a generic characteristic of these scenarios is that they establish a connection between the effective Δm^2 in the Sun and the absolute neutrino mass scale. This does not lead to any new allowed region in the oscillation parameter space. On the contrary, due to this effect, the description of solar neutrino data worsens for large absolute mass. As a consequence a lower bound on the level of degeneracy can be derived from the combined analysis of the solar and KamLAND data. In particular this implies that the analysis favours normal over inverted mass orderings. These results, in combination with a positive independent determination of the absolute neutrino mass, can be used as a test of these scenarios together with a precise determination of the energy dependence of the survival probability of solar neutrinos, in particular for low energies.

*Electronic address: marco.cirelli@yale.edu

[†]Electronic address: concha@insti.physics.sunysb.edu

[‡]Electronic address: penya@ias.edu

I. INTRODUCTION

Ref. [1] recently discussed the possibility that mass varying neutrinos (MaVaNs) can behave as a negative pressure fluid which contributes to the origin of the cosmic acceleration. In particular the authors consider a scenario in which the neutrino mass arises from the interaction with a scalar field, the acceleron \mathcal{A} , whose effective potential changes as a function of the neutrino density. This establishes a very intriguing connection between two recent pieces of evidence for New Physics –the indirect observation of Dark Energy and the confirmation of neutrino masses and oscillations– that are both suggestively characterized by a similar mass scale. Besides the possible interesting cosmological effects [1, 2], from the point of view of neutrino oscillation phenomenology the unavoidable consequence of this scenario is that the neutrino mass depends on the local neutrino density and therefore can be different in media with high neutrino densities such as the Sun.

A subsequent work Ref. [3] also investigated the possibility that neutrino masses depend on the visible matter density as well. Such a dependence would be induced by non-renormalizable operators which would couple the acceleron also to the visible matter and could lead to interesting phenomenological consequences for neutrino oscillations [3, 4, 5]. However, unlike the dependence on the local neutrino density, which is an unavoidable consequence of the proposed MaVaNs mechanism, the possible dependence on the visible matter density is strongly model-dependent. In principle it could be vanishingly small since so far the only information on the effective acceleron-matter couplings are upper bounds from tests on the gravitational inverse square law.

Consequently, in this work we concentrate on the phenomenological consequences associated to the unavoidable dependence of MaVaNs on the neutrino density in the Sun. We find that a generic feature of these scenarios is that they establish a connection between the effective Δm^2 in the Sun and the absolute neutrino mass scale m_{01} . Due to this effect, the description of solar neutrino data worsens for large m_{01} . In other words, a lower bound on the level of degeneracy $\Delta m_{21,0}^2/m_{01}^2$ can be derived from the combined analysis of the solar [6, 7, 8, 9, 10] and KamLAND data [11]. For the realization considered in this work, the 3σ bound is $\Delta m_{21,0}^2/m_{01}^2 > 1$ from the analysis of solar plus KamLAND data. In particular this implies that these scenarios favour normal mass orderings as for inverse mass orderings $m_{01}^2 \simeq \Delta m_{\text{ATM}}^2 \gtrsim 10^{-3} \text{ eV}^2$ which already implies $\Delta m_{21,0}^2/m_{01}^2 \lesssim 0.1$. Conversely, the constraint on m_{01} will allow a test of the validity of these scenarios in the event of a positive determination of the absolute neutrino mass scale from independent means.

The outline of the paper is as follows. In Sec. II we evaluate the density profile of neutrinos in the Sun in the SSM and discuss the results on the expected size of the neutrino mass shift induced for different forms of the scalar potential. Section III contains our results for the effective neutrino mass splitting in the Sun and the modification of the solar neutrino survival probability. Finally in Sec. IV we illustrate the generic quantitative consequences of these scenarios by presenting the results of an analysis of solar (plus KamLAND) data

for a particular realization.

II. MASS VARYING SOLAR NEUTRINOS

For most purposes in this section, the derivation of the effective neutrino mass in the presence of the solar neutrino background can be made in a model independent way using the neutrino mass m_ν as the dynamical field (without making explicit use of the dependence of m_ν on the accelaron field \mathcal{A}).

In this approach at low energies the effective Lagrangian for m_ν is

$$\mathcal{L} = m_\nu \bar{\nu}^c \nu + V_{tot}(m_\nu), \quad (1)$$

where $V_{tot}(m_\nu) = V_\nu(m_\nu) + V_0(m_\nu)$ contains the contribution to the energy density both from the neutrinos as well as from the scalar potential. The condition of minimization of V_{tot} determines the physical neutrino mass.

The contribution of a neutrino background to the energy density is given by

$$V_\nu = \int \frac{d^3k}{(2\pi)^3} \sqrt{k^2 + m_\nu^2} f(k), \quad (2)$$

where $f(k)$ is the sum of the neutrino and antineutrino occupation numbers for momentum k . V_ν receives contribution from the cosmological Big Bang remnant neutrinos as well as from any other neutrinos that might be present in the medium. Thus in general

$$V_\nu(m_\nu) = V_{C\nu B} + V_{\nu, \text{medium}} = m_\nu n^{C\nu B} + V_{\nu, \text{medium}}, \quad (3)$$

where we have used that in the present epoch relic neutrinos are non relativistic. $n^{C\nu B} = 112 \text{ cm}^{-3}$ for each neutrino species. In a medium like the Sun, which contains an additional background of relativistic neutrinos, $V_{\nu, \text{medium}}$ is given by Eq. (2). Notice that in writing Eq. (2) we have neglected the possible dependance of the neutrino mass on the ordinary matter density, mediated by the accelaron field [3]. In the language of [3], this implies that we are assuming that $\lambda_B \ll 10^{-3}$, where λ_B is the coupling of the scalar field with baryonic matter.

Thus in the Sun, the condition of minimum of the effective potential reads

$$\left. \frac{\partial V_{tot}(m_\nu)}{\partial m_\nu} \right|_{m_\nu} = 0 \quad \Rightarrow \quad V'_0(m_\nu) + n^{C\nu B} (1 + m_\nu A) = 0, \quad (4)$$

where we have defined the average inverse energy parameter normalized to the CMB neutrino density

$$A \equiv \frac{1}{n^{C\nu B}} \int \frac{d^3k}{(2\pi)^3} \frac{1}{\sqrt{k^2 + m_\nu^2}} f_{\text{Sun}}(k). \quad (5)$$

In the SSM the distribution of relativistic electron neutrino sources in the Sun is assumed to be spherically symmetric and it is described in terms of radial distributions $p_i(r)$ for $i = pp$,

${}^7\text{Be}$, N , O , pep , F , and ${}^8\text{B}$ fluxes. As a consequence, the density of neutrinos in the Sun is only a function of the distance from the center of the Sun, x . It is computed integrating over the contributions at point x due to the neutrinos isotropically emitted by each point source, as:

$$n^{\text{Sun}}(x) = \sum_i K_i \frac{2\pi}{x} \int dr r \log \frac{x+r}{|x-r|} p_i(r). \quad (6)$$

K_i are constants determined by normalization to the observed neutrino fluxes at the location of the Earth as:

$$\begin{aligned} n^{\text{Sun}}(x) &= \sum_i \frac{(1\text{AU})^2}{2R_\odot^2} \frac{1}{x} \frac{\Phi_{\nu,i}}{c} \int dr 4\pi r \log \frac{x+r}{|x-r|} p_i(r) \\ &= 4.6 \times 10^4 \text{ cm}^{-3} \frac{1}{x} \sum_i \alpha_i \int dr 4\pi r \log \frac{x+r}{|x-r|} p_i(r). \end{aligned} \quad (7)$$

Both r and z are given in units of R_\odot so $\int_0^1 4\pi r^2 p_i(r) = 1$ and $\alpha_i = \Phi_{\nu,i}/\Phi_{\nu,pp}$. We use in our calculations the fluxes from Bahcall, Serenelli and Basu 2005 BS05(OP) [13], and the corresponding production point distributions $p_i(r)$ [14].

Altogether we get the density of relativistic neutrinos in the Sun shown in Fig. 1. As seen in the figure the neutrino density is maximum at the center of the Sun where it reaches $2.2 \times 10^7/\text{cm}^3$. It decreases by over two orders of magnitude at the edge of the Sun.

Correspondingly we find their average inverse energy parameter normalized to the CMB neutrino density (5)

$$A(x) = 0.00186 \text{ eV}^{-1} \frac{1}{x} \sum f_i \int dr 4\pi r \log \frac{x+r}{|x-r|} p_i(r), \quad (8)$$

where we have used

$$\int dE \frac{1}{E} \frac{d\Phi_{pp}}{dE}(E) = 2.7 \times 10^5 \text{ cm}^{-2} \text{ s}^{-1} \text{ eV}^{-1}, \quad (9)$$

and $f_i = \frac{\int dE \frac{1}{E} \frac{d\Phi_{\nu,i}}{dE}}{\int dE \frac{1}{E} \frac{d\Phi_{\nu,pp}}{dE}} = 2.3 \times 10^{-2}, 2 \times 10^{-3}, 1 \times 10^{-3}, 3.6 \times 10^{-4}, 2.7 \times 10^{-5}$, and 4×10^{-6} give the small relative contribution from the ${}^7\text{Be}$, N , O , pep , F , and ${}^8\text{B}$ fluxes. In deriving Eq.(8) we have neglected the neutrino mass with respect to its characteristic energy in the Sun.

In Fig. 1 we plot the factor $A(x)$ in Eq.(8). As seen in the figure $A(x) \sim \mathcal{O}(1) \text{ eV}^{-1}$ in the region of maximum density, as expected, since $A \sim (n^{\text{sun}}/n^{C\nu B})(1/\langle E_\nu \rangle)$ with $\langle E_\nu \rangle \sim 0.1 \text{ MeV}$ being the characteristic pp neutrino energy. The size of A is what makes the effect so relevant for solar neutrinos. Let us comment that Eq.(8) is obtained under the approximation that the energy spectrum of the neutrinos is independent of the production point. This is a very good approximation since the temperature inside the production region is known to vary only within a factor ~ 3 ($T \sim 5\text{--}15 \text{ } 10^6 \text{ K}$) which corresponds to energy variations of the order of keV. An extreme upper bound to the expected corrections due to

departures from this approximation can be obtained from the results of Ref. [15]. In that work the shapes of the different neutrino spectra in the solar interior and in the laboratory were compared and the corrections found were of the order $\mathcal{O}(10^{-5})$ for beta decay neutrino spectra and at most 1% for the pp neutrino spectrum.

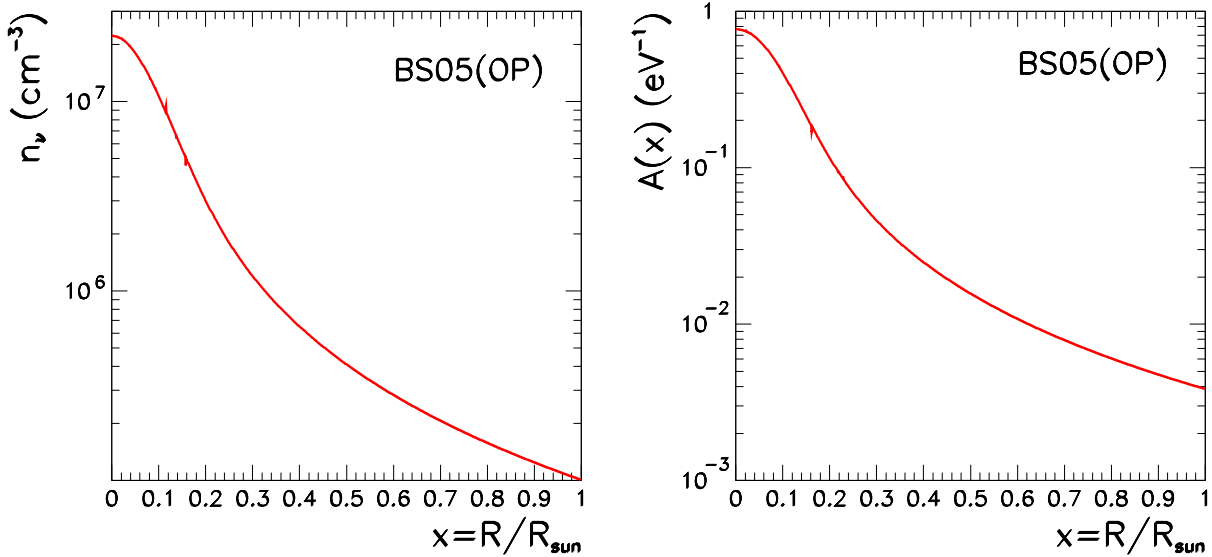


FIG. 1: Density of relativistic neutrinos in the Sun and the corresponding A factor as a function of the distance from the center of the Sun.

Solving Eq. (4) with the $A(x)$ term above one finds the effective value of the neutrino mass as a function of the solar neutrino density, while the vacuum neutrino mass m_ν^0 can be found from the corresponding condition outside of any non-relic neutrino background

$$\left. \frac{\partial V_{\text{tot}}(m_\nu)}{\partial m_\nu} \right|_{m_\nu^0} = 0 \quad \Rightarrow \quad V_0'(m_\nu^0) + n^{C\nu B} = 0. \quad (10)$$

It is clear from Eqs. (4) and (10) that the precise shift induced in the neutrino mass by the presence of an additional neutrino density depends on the exact form of the scalar potential $V_0(m_\nu)$. In general one can parametrize the scalar potential as

$$V_0(m_\nu) = \Lambda^4 f\left(\frac{m_\nu}{\mu}\right), \quad (11)$$

factoring out an overall scale Λ^4 which would set the scale of the cosmological constant in a standard scenario and a function f which depends on the dimensionless ratio m_ν/μ , where μ is an accessory mass scale which will have no particular role for our discussion.

The observation that the equation of state for the dark energy,

$$\omega + 1 = -\frac{m_\nu^0 V_0'(m_\nu^0)}{V_{\text{tot}}(m_\nu^0)},$$

must have $\omega \approx -1$ (e.g. $-1.21 < \omega < -0.88$ at 68% c.l. combining the cosmological data sets [16]) implies that the scalar potential must be fairly flat

$$\frac{dV_0(m_\nu)}{dm_\nu} \ll 1. \quad (12)$$

Furthermore Eq. (10) implies

$$\frac{dV_0(m_\nu)}{dm_\nu} < 0, \quad (13)$$

this is, the potential must be a monotonically decreasing function of m_ν .

Given the requirements (12) and (13) three suitable paradigmatic forms of the function $f(m_\nu/\mu)$ have been proposed [1, 2].

(i) A *logarithmic* form

$$f\left(\frac{m_\nu}{\mu}\right) = \log\left(\frac{\mu}{m_\nu}\right). \quad (14)$$

In this case from Eqs. (4) and (10) one gets the equation for the neutrino mass shift

$$m_\nu - m_\nu^0 = -A m_\nu^2 \quad (15)$$

whose solution in the limit of small A is

$$m_\nu = m_\nu^0 - A(m_\nu^0)^2 + \dots \quad (16)$$

Eq. (15) shows explicitly that the relative shift in the neutrino mass due to the additional neutrino background $(m_\nu - m_\nu^0)/m_\nu$ grows in magnitude with the neutrino mass scale.

(ii) A *power law* with a small fractionally power

$$f\left(\frac{m_\nu}{\mu}\right) = \left(\frac{m_\nu}{\mu}\right)^{-\alpha} \quad (\alpha > 0). \quad (17)$$

The condition $\omega \approx -1$ implies $\alpha \ll 1$ and one gets

$$m_\nu - (m_\nu^0)^{\alpha+1} m_\nu^{-\alpha} = -A m_\nu^2, \quad (18)$$

which for $\alpha \ll 1$ is the same as Eq.(15).

(iii) An *inverse exponential*

$$f\left(\frac{m_\nu}{\mu}\right) = e^{\frac{\mu}{m_\nu}}, \quad (19)$$

implies

$$m_\nu - m_\nu^0 \left(\frac{m_\nu^0}{m_\nu} \exp \left[-\frac{\omega + 1}{\omega} \left(\frac{m_\nu^0}{m_\nu} - 1 \right) \right] \right) = -A m_\nu^2, \quad (20)$$

which in the limit $\omega \rightarrow -1$ gives a cubic equation in m_ν

$$m_\nu^2 - (m_\nu^0)^2 = -A m_\nu^3, \quad (21)$$

whose exact solution for small A is

$$m_\nu = m_\nu^0 - \frac{A}{2}(m_\nu^0)^2 + \dots, \quad (22)$$

to be compared with Eq.(16).

In summary within choices of the scalar potential which verify the conditions of flatness and monotony the relative shift in the neutrino mass value due to the solar neutrino density background grows with the neutrino mass while the exact value of the shift is only moderately model dependent.

III. MASS VARYING NEUTRINO OSCILLATIONS IN THE SUN

The discussion in the previous section applies to one neutrino species. In order to determine the effect of the scenario on the solar neutrino oscillations we need to extend it to two or more neutrinos. This rises the issue of how many neutrino states do acquire a contribution to their mass via the coupling to the acceleron field. In principle with one acceleron field, only one combination of the different $m_{\nu_i} \equiv m_i$ has to be taken to be the dynamical field for the purpose of analyzing the minimal energy density.

Notwithstanding, in the following discussion we are going to assume that all neutrinos acquire a contribution to their mass via the couplings to the dark sector and that such contributions are independent¹.

In this case we can simply write the effective Lagrangian for the neutrinos as

$$\mathcal{L} = \sum_i m_i \bar{\nu}_i^c \nu_i + \sum_i [m_i n_i^{C\nu B} + V_{\nu_i, \text{medium}} + V_0(m_i)] , \quad (23)$$

and the condition of minimum of the effective potential implies that it has to be verified that

$$\frac{dV_0(m_i)}{dm_i} + n_i^{C\nu B} + m_i \int \frac{d^3k}{(2\pi)^3} \frac{1}{\sqrt{k^2 + m_i^2}} f_{\text{Sun},i}(k) = 0, \quad (24)$$

for each m_i independently. Under this assumption, the coupling to the dark sector leads to a shift of the neutrino masses but does not alter the leptonic flavour structure which is determined either by other non-dark contributions to the neutrino mass or from the charged lepton sector of the theory. We will go back to this point after presenting the results.

For the sake of concreteness we will present our results on solar neutrinos oscillations for the case of a logarithmic potential $V_0(m_i) = \Lambda^4 \log(\mu/m_i)$. In this case Eqs.(24) lead to three (one for each neutrino) independent equations for the mass shifts

$$(m_i - m_i^0) = -m_i^2 A_i, \quad (25)$$

¹ A trivial realization of such scenario is to introduce several stable acceleron fields which couple independently to the different neutrino states.

where

$$A_i = \frac{1}{n_i^{C\nu B}} \int \frac{d^3k}{(2\pi)^3} \frac{1}{\sqrt{k^2 + m_i^2}} f_{\text{Sun},i}(k). \quad (26)$$

So even in this case of no leptonic mixing from the scalar potential, there is a generation dependence of the A factor from the flavour dependence of the background neutrino density.

We assume that all massive neutrinos have the same contribution to the cosmic density, $n_i^{C\nu B} = 112 \text{ cm}^{-3}$ for all i . In this case the generation dependence comes from the fact that in the Sun only ν_e 's are produced. Using the standard labeling of the massive neutrino states and neglecting θ_{13} we find only the states ν_1 and ν_2 have their masses modified by the presence of the solar neutrino background as given in Eq. (15) with

$$\begin{aligned} n_1(x) &= \cos^2 \theta_{12}^V n_{\nu_e}(x) \Rightarrow A_1(x) = \cos^2 \theta_{12}^V A(x), \\ n_2(x) &= \sin^2 \theta_{12}^V n_{\nu_e}(x) \Rightarrow A_2(x) = \sin^2 \theta_{12}^V A(x), \end{aligned} \quad (27)$$

where θ_{12}^V is the vacuum mixing angle and $A(x)$ is given in Eq.(8).

Altogether this implies that the effective ‘‘kinetic’’ (we label it kinetic to make it explicit that it does not contain the MSW potential) mass difference in the Sun is

$$\Delta m_{\text{kin}}^2(x) = m_2^2(x) - m_1^2(x) \simeq \Delta m_{21,0}^2 [1 - 3A_2(x)m_{01}] + 2[A_1(x) - A_2(x)]m_{01}^3 + \dots \quad (28)$$

where, for clarity, we have given the explicit expression when expanded in powers of $A(x)$ and the neutrino mass scale m_{01} . $\Delta m_{21,0}^2 = m_{02}^2 - m_{01}^2$ and θ_{12}^V are ‘‘vacuum’’ mass difference and mixing angle. These are the parameters measured with reactor antineutrinos at KamLAND². In Fig. 2 we plot the effective $\Delta m_{\text{kin}}^2(x)$ as a function of the distance from the center of the Sun for different values of the neutrino mass scale m_{01} . In this figure, and it what follows the results with $m_{01} = 0$ are obtained by zeroing the dark-energy contributions so $\Delta m_{\text{kin}}^2(x) = \Delta m_{21,0}^2$. Strictly speaking our derivation of $\Delta m_{\text{kin}}^2(x)$ assumes that all CMB neutrinos are non-relativistic in the present epoch, an assumption which does not hold for the lightest neutrino if $m_{01} = 0$. But as long as the behaviour is continuous, the contribution will be negligible small for this case.

From Eq.(28) we read that, as long as the different massive neutrinos have different projections over ν_e ($A_1 \neq A_2$), $\Delta m_{\text{kin}}^2(x)$ receives a contribution from the solar neutrino background which rapidly grows with the neutrino mass scale m_{01} . For the particular scenario that we are studying $A_1(x) - A_2(x) = \cos 2\theta_{12}^V A(x) > 0$ so the effective kinetic mass splitting is positive and larger than the vacuum one in the resonant side for neutrinos .

² We estimate an A factor from the background density of reactor antineutrino and geoneutrinos to be of the order of $\mathcal{O}(10^{-11} \text{ eV}^{-1})$. This includes geoneutrinos from radioactive elements yielding (anti)neutrinos that are under the threshold of running experiments but actually give the dominant contribution to this A factor.

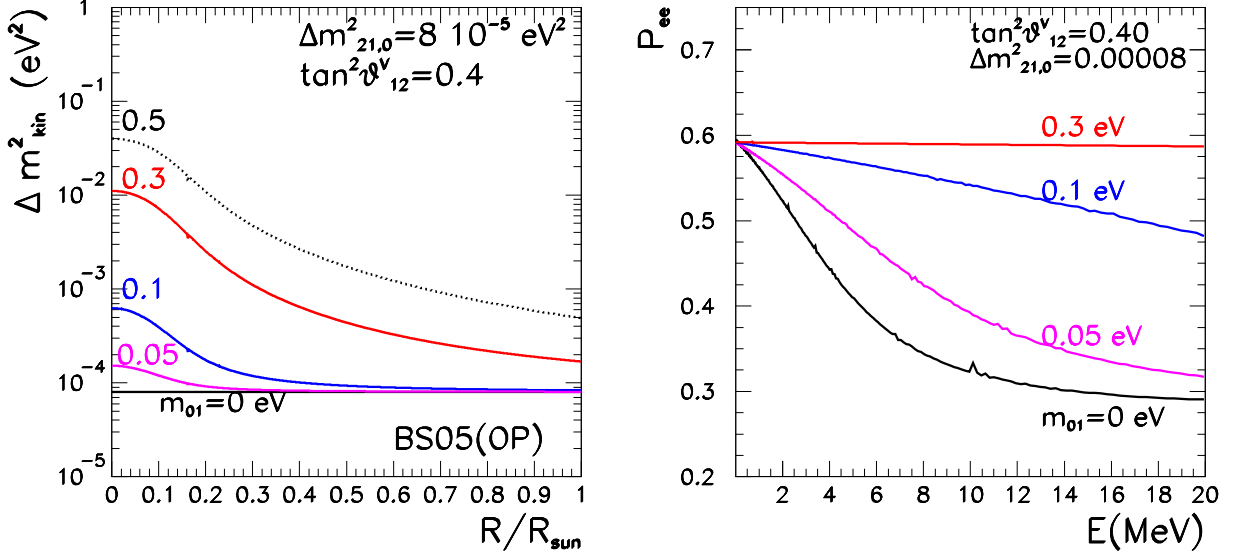


FIG. 2: (Left) Effective mass difference in the Sun. (Right) Survival probability of solar ν_e 's as a function of the neutrino energy. This survival probability has been obtained for neutrinos produced around $x = 0.05$ as it is characteristic of ${}^8\text{B}$ neutrinos.

Next we evaluate the corresponding survival probability for solar MaVaNs by solving the evolution equations

$$i \frac{d}{dx} \begin{pmatrix} \nu_e \\ \nu_\mu \end{pmatrix} = \left[\frac{1}{2E} U \begin{pmatrix} 0 & 0 \\ 0 & \Delta m_{\text{kin}}^2(x) \end{pmatrix} U^\dagger + \begin{pmatrix} V(x) & 0 \\ 0 & 0 \end{pmatrix} \right] \begin{pmatrix} \nu_e \\ \nu_\mu \end{pmatrix}. \quad (29)$$

where $V(x) = \sqrt{2} G_F N_e(x)$ is the MSW potential [17]. We need not include MSW-like modifications induced by an effective one loop coupling neutrino-electron mediated by the acceleron, because these can be seen to be negligibly small under mild assumptions, as discussed in [1, 3]. U is the mixing matrix of angle θ_{12}^V . We solve this equation by numerical integration along the neutrino trajectory. However in most of the parameter space the evolution of the neutrino system is adiabatic and the survival probability is very well reproduced by the standard formula

$$P_{ee} = \frac{1}{2} + \frac{1}{2} \cos 2\tilde{\theta}_{12,0} \cos 2\theta_{12}^V, \quad (30)$$

where $\tilde{\theta}_{12,0}$ is the effective mixing angle at the neutrino production point x_0 . It includes both the effect of the point dependent kinetic mass splitting as well as the effect of the MSW potential.

$$\cos 2\tilde{\theta}_{12,0} = \frac{\Delta m_{\text{kin}}^2(x_0) \cos 2\theta_{12}^V - A_{\text{MSW}}(x_0)}{\sqrt{(\Delta m_{\text{kin}}^2(x_0) \cos 2\theta_{12}^V - A_{\text{MSW}}(x_0))^2 + (\Delta m_{\text{kin}}^2(x_0) \sin 2\theta_{12}^V)^2}} \quad (31)$$

where $A_{\text{MSW}}(x_0) = 2EV(x_0)$.

We plot in Fig. 2 the survival probability as a function of the neutrino energy for $\Delta m_{21,0}^2 = 8 \times 10^{-5} \text{ eV}^2$ and $\tan^2 \theta_{12}^V = 0.4$ and different values of the neutrino mass scale m_{01} . As can be seen in the figure, due to the different contributions of the solar neutrino background to the two mass eigenstates, the energy dependence of the survival probability is rapidly damped even for mildly degenerated neutrinos. As a consequence, in these cases, it is not possible to simultaneously accommodate the observed event rates in solar neutrino experiments [6, 7, 8, 9, 10] and in KamLAND [11] as we quantify next.

IV. CONSTRAINTS FROM SOLAR NEUTRINO OBSERVABLES

We present in this section the results of the global analysis of solar and KamLAND data in the framework of MaVaNs for the specific realization discussed in the previous section.

Details of our solar neutrino analyses have been described in previous papers [18, 19]. The solar neutrino data we use includes the Gallium [7, 8] (averaged to 1 data point) and Chlorine [6] (1 data point) radiochemical rates, the Super-Kamiokande [9] zenith spectrum (44 bins), and SNO data previously reported for phase 1 and phase 2. The SNO data used consists of the total day-night spectrum measured in the pure D₂O phase (34 data points), plus the total charged current (CC, 1 data point), electron scattering (ES, 1 data point), and neutral current (NC, 1 data point) rates measured in the salt phase [10]. The main difference with respect to previous analysis is that we use the solar fluxes from Bahcall, Serenelli and Basu 2005 [13] but we still allow the normalization of the ⁸B flux to be a free parameter to be fitted to the data.

The analysis of solar neutrino depends then of 4 parameters $\Delta m_{21,0}^2$, $\tan^2 \theta_{12}^V$, m_{01} , and f_B (the reduced flux f_B , is defined as the ⁸B solar neutrino flux divided by the corresponding value predicted by the BS05 standard solar model).

We show in the left panels of Fig. 3 the result of the global analysis of solar data in the form of the allowed regions in the 3-dimensional parameter space of $\Delta m_{21,0}^2$, $\tan^2 \theta_{12}^V$, m_{01} , after marginalization over the f_B . The regions have been defined by the conditions $\Delta \chi_{\text{sol}}^2(\Delta m_{21,0}^2, \theta_{21}^V, m_{01}) \equiv \chi_{\text{min},f_B}^2(\Delta m_{21,0}^2, \theta_{21}^V, m_{01}) - \chi_{\text{min}}^2 \leq \Delta \chi^2(\text{C.L.}, 3 \text{ d.o.f.})$, where $\Delta \chi^2(\text{C.L.}, 3 \text{ d.o.f.}) = 6.25, 7.81, 11.34, \text{ and } 14.16$ for C.L. = 90%, 95%, 99% and 99.73% (3σ) respectively, and χ_{min}^2 is the global minimum which is obtained for the totally hierarchical case $m_{01} = 0 \text{ eV}$ and $\Delta m_{21,0}^2 = 6.9 \times 10^{-5} \text{ eV}^2$, $\tan^2 \theta_{12}^V = 0.4$ and $f_B = 0.92$.

In the figure we plot sections of the 3-dimensional allowed regions at fixed values of m_{01} . As seen in the figure, as m_{01} increases the allowed region of the solar analysis shifts to lower values of $\Delta m_{21,0}^2$ to compensate for the increase of Δm_{kin}^2 and the fit to solar data worsens. The worsening is driven by two main effects. First, the increase of the survival probability of ⁸B neutrinos makes more difficult to accommodate the observed CC/NC ratio (and CC/ES) at SNO. In principle the CC rate could be cured by the free ⁸B flux f_B , but the NC constrains the allowed values of f_B . Second, shifting to lower values of $\Delta m_{21,0}^2$ increases the expected

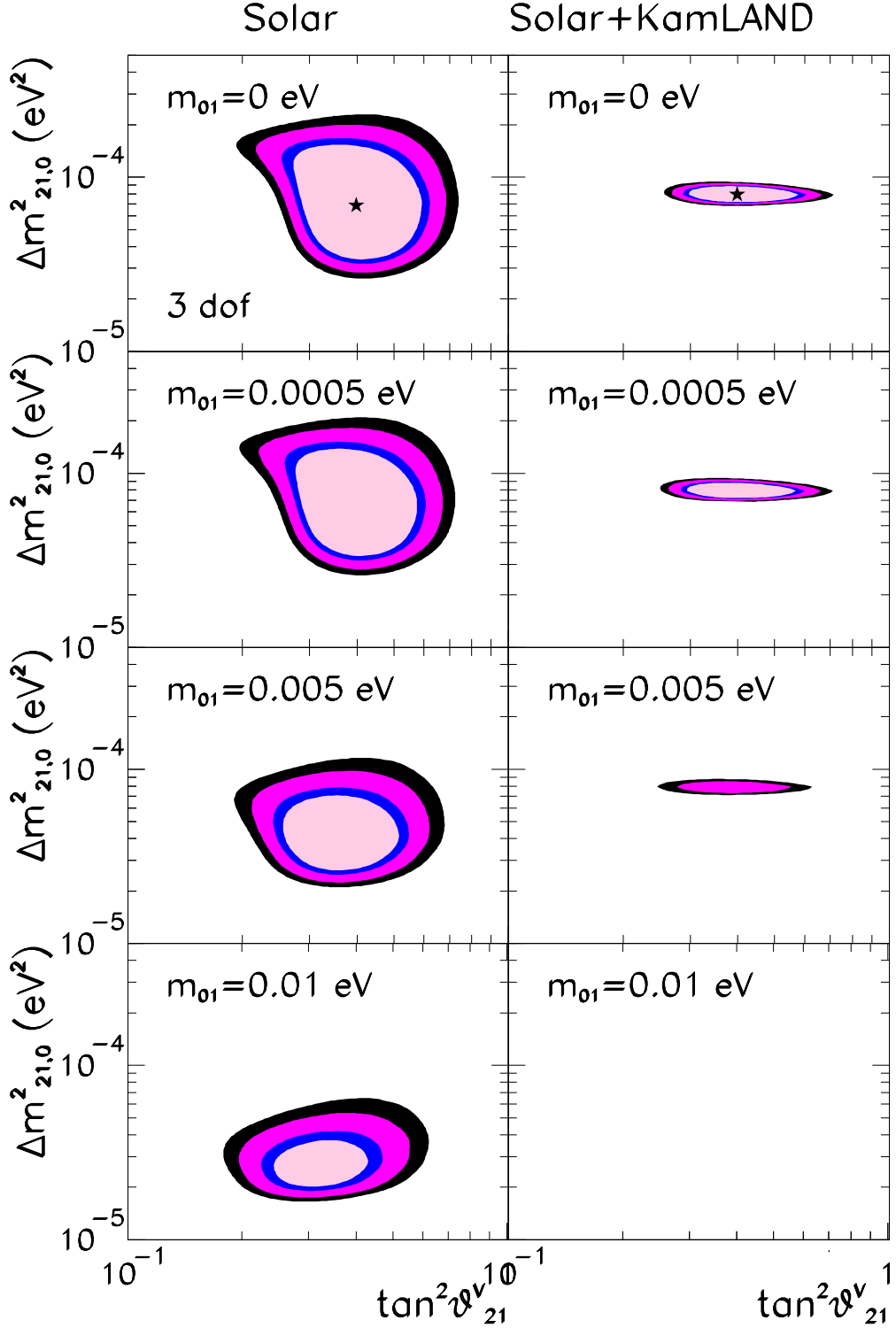


FIG. 3: Allowed regions from the global analysis of solar and solar plus KamLAND data in the $(\Delta m_{21,0}^2, \tan^2 \theta_{12}^V, m_{01})$ parameter space, shown for 4 sections at fixed values of m_{01} . The different contours corresponds to 90%, 95%, 99%, and 3σ CL for 3dof. The global minima are marked with a star.

day-night asymmetry. This eventually makes the agreement with the data impossible for high enough values of m_{01} since the neutrino density in the Earth is too small to induce any additional effect on the day-night asymmetry. Consequently, we find that the 3-dimensional region at 3σ extends only to $m_{01} \leq 0.05$ eV.

It is clear from these results, that the fit for large values of m_{01} will become worse after combination with the KamLAND data. In the present framework the analysis of KamLAND only depends on the “vacuum” parameters $\Delta m_{21,0}^2$ and $\tan^2 \theta_{21}^V$. We include here the results of a likelihood analysis to the unbinned KamLAND data [12]. Details of this analysis will be presented elsewhere [20].

We show in the right panels of Fig. 3 the result of the combined analysis of solar plus KamLAND. The global minimum is obtained for the totally hierarchical case $m_{01} = 0$ eV and $\Delta m_{21,0}^2 = 7.9 \times 10^{-5}$ eV², $\tan^2 \theta_{12}^V = 0.4$ and $f_B = 0.90$. As seen in the figure as m_{01} increases the allowed region becomes smaller. As a matter of fact, due to the shift of the solar region to lower values of $\Delta m_{21,0}^2$, the local best fit point of the combined analysis moves to the LMA0 region [21] for “intermediate” values of $m_{01} \sim \mathcal{O}(10^{-2})$ eV. In other words, for those values, LMA0 becomes less disfavoured than in the hierarchical case. For example for $m_{01} = 0$ the LMA0 region lies at $\Delta\chi^2 = 37.5$, which implies that it would be part of the 3-dim allowed region at 5.5σ , while for $m_{01} = 0.01$ eV the LMA0 region lies at $\Delta\chi^2 = 15.3$ and it would be part of the 3-dim region at allowed at 3.15σ .

The result of the previous discussion is that generically MaVaN’s imply that the description of solar data worsens with the degree of degeneracy of the neutrinos. In order to quantify this statement in the present scenario, we define the “degeneracy parameter”, $x_{\text{deg}} \equiv \Delta m_{21,0}^2/m_{01}^2$, and study the dependence of χ^2 on this parameter after marginalization over all others:

$$\Delta\chi_{\text{sol}(\text{glob})}^2(x_{\text{deg}}) = \min_{\chi_{\text{sol}(\text{glob})}^2}(\Delta m_{21,0}^2, \theta_{12}^V, m_{01}, f_B | x_{\text{deg}} = \Delta m_{21,0}^2/m_{01}^2) - \chi_{\text{min},\text{sol}(\text{glob})}^2. \quad (32)$$

In Fig. 4 we plot $\Delta\chi_{\text{sol}(\text{glob})}^2(x_{\text{deg}})$. Within the present bounds on the absolute neutrino mass [22], $2 \times 10^{-5} \lesssim x_{\text{gen}} < \infty$. As discussed above, we find that for the considered scenario of MaVaN’s, the best fit occurs for hierarchical neutrinos $x_{\text{deg}} = \infty$ while the fit becomes worse as the neutrinos become more degenerate. As seen in the figure, the curve for the solar plus KamLAND analysis is not monotonic but presents a secondary minimum around $x_{\text{deg}} = 0.1$. This is due to the migration of the local best fit point to the LMA0 region for values of $m_{01} \sim \mathcal{O}(10^{-2})$ eV.

Quantitatively, we find the lower bound at 3σ :

$$x_{\text{deg}} > 2 \times 10^{-2} (1), \quad (33)$$

from the analysis of solar (solar plus KamLAND) data. In particular, this bound implies that in this scenario inverted mass ordering is disfavoured since in this case $m_{01}^2 \simeq \Delta m_{\text{ATM}}^2 \gtrsim 10^{-3}$ eV² which implies $x_{\text{deg}} \lesssim 0.1$.

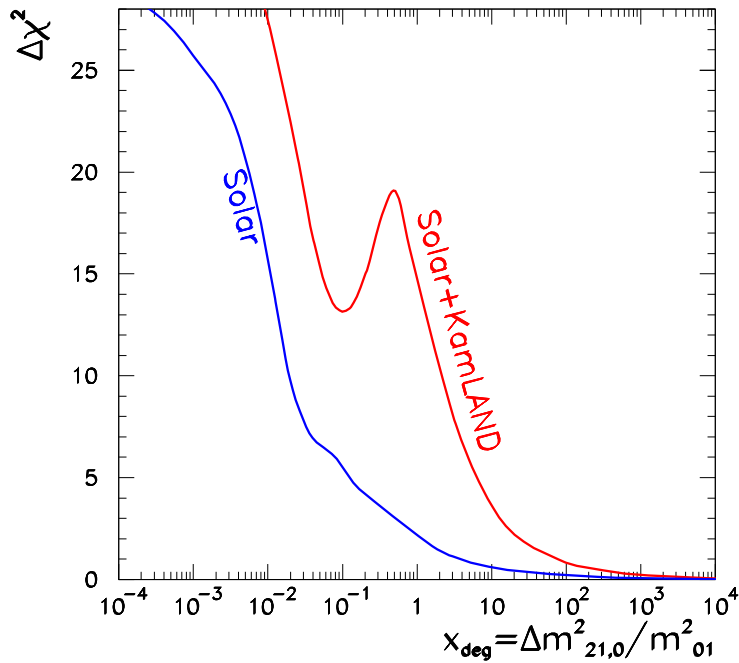


FIG. 4: Dependence of $\Delta\chi^2$ on the degeneracy parameter $\Delta m_{21,0}^2/m_{01}^2$ from the global analysis of solar and solar plus KamLAND data after marginalization in all other parameters.

Finally we want to comment on the possible model-dependence of these results. As discussed in the previous sections there are two main sources of arbitrariness in our derivations: the choice of the functional form of the scalar potential, and the assumption that all neutrinos acquire an independent contribution to their mass via the couplings to the dark sector with no generation mixing.

As shown in our discussion in Sec. II the choice of the potential may affect the exact form of the equation relating $\Delta m_{21,0}^2$ to $\Delta m_{kin}^2(x)$ but it will not alter the fact that $\Delta m_{kin}^2(x)$ grows with the neutrino mass scale. In particular choosing a power law potential with a small fractionally power $\alpha \ll 1$ yields the same results while the results for an inverse exponential potential are very similar but for a slightly higher value of m_{01} .

Concerning the assumption of no generation mixing from the dark sector contribution to the neutrino mass, its effect can be understood as follows. In general, if the couplings to the dark sector are not “mass-diagonal” they will induce an additional source of rotation between the flavour eigenstates and the effective mass eigenstates. This would imply that the mixing angle in Eq.(28) would not be θ_{12}^V but some $\theta_{12}^{kin}(x)$. In general the qualitative features of the results will still be valid although the quantitative bounds will obviously vary. In particular, the bounds will become tighter if the mixing could be such that the mass eigenstates were inverted ($\theta_{12}^{kin}(x) > \pi/4$).

A possible exception to this general argument would be the special case in which the

flavour structure of the potential is such that $A_2(x) \simeq A_1(x)$ without a substantial modification of θ_{12} . In this case the $A_2(x) - A_1(x)$ term in Eq. (28) would be suppressed and the shift on Δm^2 would be small even for $m_{01} \sim 2$ eV. This would imply $\Delta m_{kin}^2(x) < \Delta m_{21,0}^2$, this effect being mostly relevant for neutrinos which are produced nearer the center of the Sun. As a consequence the survival probability for ${}^7\text{B}$ neutrinos can be slightly lower and a slightly better fit to the data could be achieved.

Summarizing, in this work we have studied the phenomenological consequences of the dependence of MaVaNs on the neutrino density in the Sun. We have evaluated the density profile of neutrinos in the Sun in the SSM and the expected size of the neutrino mass shift induced for different forms of the scalar potential. We find that generically these scenarios establish a connection between the effective mass splitting in the Sun and the absolute neutrino mass scale. We have analyzed the quantitative consequences of this effect, by performing a global analysis to solar and KamLAND data for a particular realization of this mechanism. Our results show that the description of solar neutrino data worsens for large neutrino mass scale and an upper bound on the absolute neutrino mass scale can be derived. Equivalently, we derive a lower bound on the level of degeneracy $\Delta m_{21,0}^2/m_{01}^2 > 2 \times 10^{-2}$ (1) from the analysis of solar (solar plus KamLAND) data. A straightforward consequence of this is that normal mass orderings are favoured over inverse mass orderings.

These results, in combination with a positive determination of the absolute neutrino mass scale from independent means, can be used as a test of these scenarios. Ultimately, these scenarios will be tested by the precise determination of the energy dependence of the survival probability of solar neutrinos, in particular for low energies [18, 23].

Acknowledgments

We thank John Bahcall, Maurizio Piai, Aldo Serenelli, and Neal Weiner for useful conversations. We are particularly indebted to A. Serenelli for discussions on the detailed production point distributions of neutrinos in the BS05 model. The work of M.C. is supported in part by the USA Department of Energy under contract DE-FG02-92ER-40704. CPG acknowledges support from the Keck Foundation and NSF grant No. PHY0354776. MCG-G is supported by National Science Foundation grant PHY0098527 and by Spanish Grant No FPA-2004-00996.

-
- [1] R. Fardon, A. E. Nelson and N. Weiner, JCAP **0410**, 005 (2004) [astro-ph/0309800]. See also P. Gu, X. Wang and X. Zhang, Phys. Rev. D **68**, 087301 (2003) [hep-ph/0307148].
- [2] R. D. Peccei, Phys. Rev. D **71**, 023527 (2005) [hep-ph/0411137]; P. Q. Hung and H. Pas, [astro-ph/0311131]; X. J. Bi, P. h. Gu, X. l. Wang and X. m. Zhang, Phys.

- Rev. D **69**, 113007 (2004) [arXiv:hep-ph/0311022]; X. J. Bi, B. Feng, H. Li and X. m. Zhang, arXiv:hep-ph/0412002; P. h. Gu and X. j. Bi, Phys. Rev. D **70**, 063511 (2004) [arXiv:hep-ph/0405092].
- [3] D. B. Kaplan, A. E. Nelson and N. Weiner, Phys. Rev. Lett. **93**, 091801 (2004) [hep-ph/0401099].
- [4] K. M. Zurek, JHEP **0410**, 058 (2004) [arXiv:hep-ph/0405141].
- [5] V. Barger, P. Huber and D. Marfatia, [arXiv:hep-ph/0502196.]
- [6] B.T. Cleveland et al., Astrophys. J. **496** (1998) 505.
- [7] C. Cattadori, *Results from radiochemical solar neutrino experiments*, talk at XXIst International Conference on Neutrino Physics and Astrophysics (NU2004), Paris, June 14–19, 2004.
- [8] GALLEX collaboration, Phys. Lett. **B 447** (1999) 127.
- [9] Super-Kamiokande Collaboration, S. Fukuda et al., Phys. Rev. Lett. **86** (2001) 5651.
- [10] SNO Collaboration, Q.R. Ahmad et al., Phys. Rev. Lett. **87** (2001) 071301; Phys. Rev. Lett. **89** (2002); Phys. Rev. Lett. **89** (2002) 011302; SNO Collaboration, S.N. Ahmed et al., Phys. Rev. Lett. **92** (2004), 181301.
- [11] KamLAND Collaboration, T. Araki *et al.*, Phys. Rev. Lett. **94**, 081801 (2005), hep-ex/0406035; KamLAND Collaboration, K. Eguchi *et al.*, Phys. Rev. Lett. **90** (2003) 021802, hep-ex/0212021.
- [12] <http://www.awa.tohoku.ac.jp/KamLAND/datarelease/2ndresult.html>
- [13] J. N. Bahcall, A. M. Serenelli and S. Basu, Astrophys. J. **621**, L85 (2005) [arXiv:astro-ph/0412440].
- [14] <http://www.sns.ias.edu/~jnb>
- [15] J. N. Bahcall, Phys. Rev. D **44**, 1644 (1991).
- [16] A. G. Riess *et al.* [Supernova Search Team Collaboration], Astrophys. J. **607**, 665 (2004) [astro-ph/0402512].
- [17] L. Wolfenstein, Phys. Rev. D **17**, 2369 (1978). Mikheyev, S.P., and A.Y. Smirnov, Yad. Fiz. **42**, 1441 (1985) [Sov. J. Nucl. Phys. **42**, 913 (1985)].
- [18] J.N. Bahcall, M.C. Gonzalez-Garcia and C. Peña-Garay, JHEP **02** (2003) 009 [hep-ph/0212147]; J.N. Bahcall and C. Peña-Garay, JHEP. **11** (2003) 004.
- [19] J. N. Bahcall, M. C. Gonzalez-Garcia and C. Pena-Garay, JHEP **0302**, 009 (2003)
- [20] C. Pena-Garay and A. Ianni in preparation.
- [21] A. Friedland, C. Lunardini and C. Pena-Garay, Phys. Lett. B **594**, 347 (2004) [arXiv:hep-ph/0402266].
- [22] J. Bonn, *et al.*, Nucl. Phys. Proc. Suppl. **91**, 273 (2001); V. M. Lobashev, *et al.* Nucl. Phys. Proc. Suppl. **91**, 280 (2001); H. V. Klapdor-Kleingrothaus, *et al.*, Eur. Phys. J. A **12**, 147 (2001).
- [23] *Low Energy Solar Neutrino Detection (LowNu2)*, ed. by Y. Suzuki, M. Nakahata, and S. Moriyama, World Scientific, River Edge, NJ, 2001.